Enhanced Seismic Performance of Moment-Resisting Frames with Non-Prismatic Beam Sections

Farid Mahmoudi, Alireza Rahai*, Farzad Hatami

Department of Civil Engineering, Amirkabir University of Technology, Tehran, Iran
* rahai@aut.ac.ir

Abstract:

Although moment-resisting frames exhibit satisfactory ductile performance, they suffer from limitations such as low stiffness. Consequently, designers attempt to enhance stiffness by reducing the span length of these frames. Meanwhile, design codes impose a minimum limit on the span-to-depth ratio for moment-resisting frames. This provision ensures the adequate formation of flexural plastic hinges at both ends of the beam. In this paper, a novel energy-absorbing steel system is proposed through numerical studies. In this system, instead of the conventional method of locally reducing beam cross-sections at both ends, a non-prismatic reduction of the beam cross-section along its entire length is introduced. As a result, energy dissipation occurs over a larger portion of the beam, thereby overcoming the aforementioned code limitation. After validation, two conventional lateral load-resisting systems and one system based on the idea presented in this study are considered, and their performance is evaluated using the finite element method. the proposed moment-resisting frame in this study exhibits approximately 2.15 times higher stiffness, twice the strength, and twice the energy absorption capacity compared to a conventional moment-resisting frame with a span-to-depth ratio of 7, while maintaining nearly equivalent plastic strain (PEEQ). Furthermore, when compared to a conventional moment-resisting frame with a span-to-depth ratio of 4 (which violates code provisions), the proposed system demonstrates comparable stiffness, strength, and energy dissipation, yet its PEEQ is about 37% lower, underscoring the superiority of the proposed concept.

Keywords: Moment resisting frame, Non-Prismatic Beam Sections, Span to depth ratio, Plastic hinge.

1. Introduction

Moment-resisting frames are widely used in structural engineering due to their adequate ductility and provision of sufficient architectural space. These frames exhibit ductile behavior owing to their effective energy absorption capacity under seismic loads. The formation of flexural plastic hinges at beam ends is the most common energy dissipation mechanism in moment-resisting frames [1]. According to seismic design codes, the clear span-to-depth ratio must exceed 5 for intermediate moment frames and 7 for special moment frames [2]. Compliance with this requirement results in shallow beam sections that often fail to resist applied loads. Consequently, this provision is frequently disregarded due to its impracticality. It should be noted that the primary reason for code-mandated minimum span-to-depth ratios is to ensure sufficient plastic hinge length at beam ends [2]. This rationale is explained below with reference to Fig 1, which compares two frames with identical sections and lateral loads but different span lengths. The plastic hinge lengths in the depicted frames are denoted as L_{p1} and L_{p2}, where plastic hinge length equals the distance between the beam end (with moment $M=ZF_y$) and the point where $M=SF_y$ (Z: plastic section modulus, F_y: steel yield stress, S: elastic section modulus). Evidently, the plastic hinge length in the shorter-span frame is insufficient, predicting poor seismic performance.

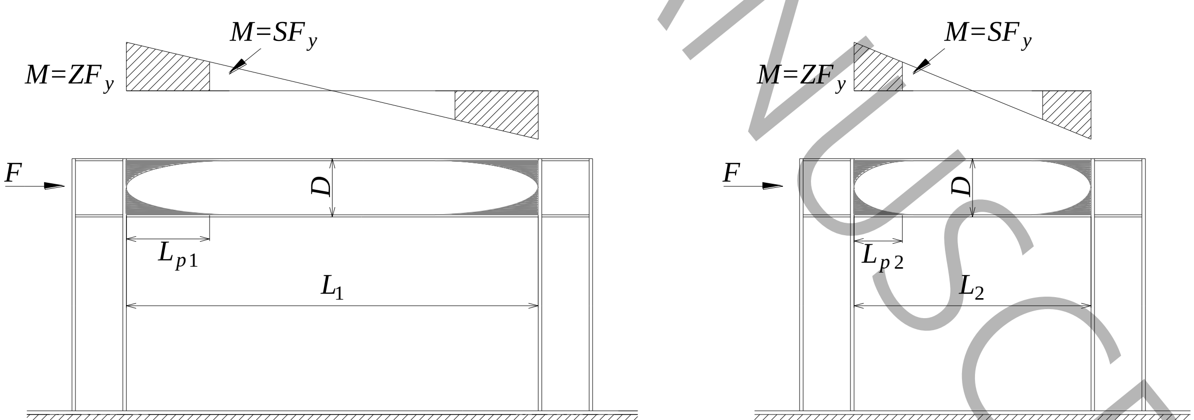

Fig 1: Bending moment diagram variation with reduced beam length in frames.

Given architecturally determined span lengths, designers must reduce beam depth to meet minimum span-to-depth requirements. Frequently, such reduced sections cannot withstand seismic displacements, leading to routine violation of this code provision. A typical example is tubular frame systems where exterior moment frames resist lateral loads while interior frames carry gravity loads [3]. Fig 2(a) illustrates a 34-story building with this system, showing closely spaced columns and deep beams [3], resulting in span-to-depth ratios as low as 4 - below the code-specified minimums of 5 and 7 for intermediate/special moment frames. Such structures are expected to perform poorly in earthquakes due to inadequate plastic hinge formation and consequent low energy absorption. Another example in Fig 2(b) shows end spans violating minimum span-to-depth requirements. Here, designers strengthened beam-column connections for protection, inadvertently exacerbating the problem by preventing proper plastic hinge formation at beam ends, resulting in unfavorable hysteretic behavior and compromised structural safety.

a) b)

Fig 2: Two moment-resisting frames with span-to-depth ratios below code limits.

To address the problems of moment-resisting frames, such as those observed in the Kobe and Northridge earthquakes, researchers introduced reduced beam sections to prevent plastic hinge formation at beam-column connections [4]. In recent years, various types of reduced sections have been proposed, including: reduced web sections [5], perforated flanges [6], double reduced sections [7], and tubular reduced sections [8]. Another approach involves strengthening beam-column connections to shift plastic hinge formation away from the joint. For example, Grami et al. [9] successfully relocated plastic hinges to the beam rather than the connection. Tree-column moment frames represent another connection-strengthening method that enhances welded joint quality [10]. This modular approach reduces material waste and improves construction efficiency [11].

Another group of studies has employed mechanical hinged connections [12] to mitigate beam-column connection failures, improving joint ductility. However, these studies still do not resolve the code-mandated span-to-depth ratio limitation. In this context, Nikoukalam and Dolatshahi [13] introduced the concept of shear-link frames, incorporating a smaller cross-section shear link at mid-span. The shear link is designed with lower capacity than the beam, enabling energy dissipation through shear yielding rather than flexural yielding, thereby bypassing the aforementioned code restriction. This concept was later refined by Dolatshahi et al. [14], [15] through perforated and layered shear links. Mahmoudi et al. [16]–[18] experimentally validated the shear-link frame idea, followed by high-rise applications by Lian et al. [19] and Guan et al. [20]. The shear link concept is generally based on intentionally weakening the beam segment (typically at the middle region of the beam in a moment-resisting frame) so that shear yielding becomes the governing inelastic mechanism instead of flexural yielding. This mechanism shifts the energy dissipation demand from bending to shear, thereby reducing the likelihood of severe flexural plastic hinges at the beam ends. One important consequence of this approach is that it may eliminate or relax the traditional limitation related to the minimum span-to-depth ratio commonly required in moment frames to ensure stable flexural yielding behavior. Furthermore, when replaceable shear links are used, the damaged link can be removed and replaced after a major earthquake, allowing the structure to be returned to service rapidly, which supports the concept of repairability and resilience in seismic design. Similarly, the perforated web approach aims to reduce the shear capacity of the beam web by introducing openings or perforations, effectively decreasing the shear stiffness and strength of the web region and again promoting controlled shear yielding over flexural yielding. In this way, the web perforations act as a predetermined “fuse” mechanism that concentrates and stabilizes inelastic shear deformations within a designated region, improving the ability of the frame to dissipate seismic energy while limiting damage to other critical components.

While recent research has addressed the span-to-depth ratio limitation, implementing solutions in buildings with low existing ratios remains challenging. Moreover, shear-link frames incur higher construction costs than conventional moment frames. Given the inherent limitations of moment-resisting frames—such as low stiffness and code restrictions—and the need for retrofitting methods, developing a novel lateral load-resisting system appears essential.

2. Research Method and Objectives

This study proposes the use of non-prismatic beam sections (NPBSs) along the beam length to address the limitations discussed earlier. Currently, the conventional approach employs reduced beam sections (RBS) only at the beam ends in moment-resisting frames. These sections are locally weakened over a specific length, confining plastic hinge formation to these regions. Fig 3(a) illustrates the traditional RBS concept, where energy dissipation occurs solely in the reduced sections. However, increasing the plastic hinge length would lead to more stable energy absorption.

Fig 3(b) demonstrates the novel system proposed in this study. Here, the beam cross-section is non-prismatically reduced starting at a specified distance from the column face. This design promotes distributed plastic hinge formation over a larger beam length under lateral loads. The setback distance from the column face prevents brittle fracture at the beam-column connection, which could cause catastrophic failure. Notably, this system is particularly suitable for tubular structural systems, where perimeter frames resist seismic loads while interior frames carry gravity loads.

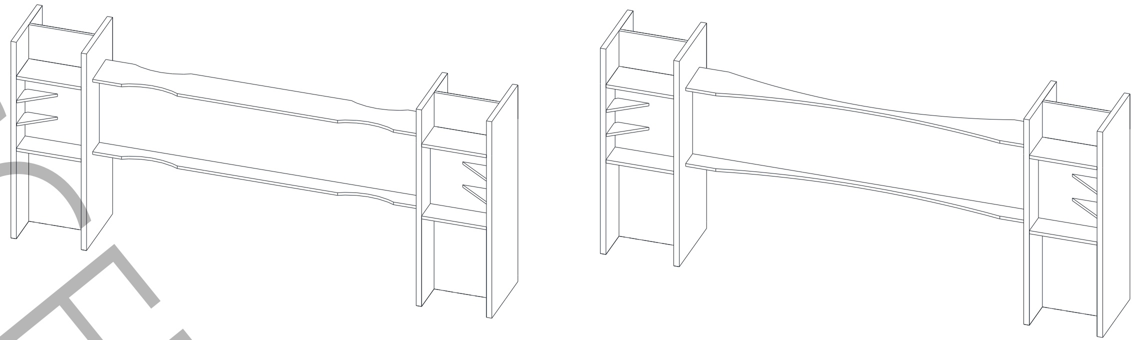

(a) Reduced beam sections at beam ends (b) Reduced beam section along the beam length

Fig 3: Moment-resisting frame configurations

The NPBS design is based on distributing flexural yielding along the beam length rather than concentrating it at the ends. As shown in Figure 1, seismic demands induce lower bending moments at the beam mid-span compared to the ends. Thus, gradually weakening the beam flanges along its length ensures near-simultaneous yielding across the entire beam under seismic loading. The design moment capacity is determined using the following equation, ensuring that nonlinear displacements are distributed along the beam rather than localized at the ends:

$$\frac{M_{p,RBS}}{Z_{RBS}} \leq \frac{M_p}{Z} \tag{1}$$

In conventional special moment frames, plastic hinges are typically assumed to form at beam ends near the beam-to-column connections. In the proposed system, however, the design objective is to promote a distributed yielding mechanism within the beam while maintaining columns and other components essentially elastic. Therefore, the plastic hinge is not concentrated at a single location; instead, it is represented as an extended plastic hinge region along the beam, effectively spanning a significant portion of the beam flange length. For a more explicit representation of hinge development in nonlinear or plastic analyses, the beam deformation model may be refined by assuming that plastic hinging initiates at the beam ends and progressively propagates toward the midspan with increasing demand. Under this assumption, the extent of the plastic hinge region can be approximately quantified based on the imposed distributed strength/stiffness reduction along the beam length, allowing a practical estimation of the evolving hinge length and an equivalent hinge location for simplified plastic analysis.

In this study, following the same methodology, three moment-resisting frame structures were designed, modeled, and analyzed using ABAQUS software [21]. Specifically, after validating the numerical model against an experimental specimen of a moment-resisting frame, the three frames under investigation were subjected to loading and evaluation. These frames include:

- A conventional moment-resisting frame with reduced beam sections (RBS) and a span-to-depth ratio of 7 (compliant with code requirements).
- A conventional moment-resisting frame with RBS and a span-to-depth ratio of 4 (violating code requirements).
- A moment-resisting frame with a non-prismatic reduced beam section along the beam length and a span-to-depth ratio of 4 (proposed system).

The first frame adheres to code-prescribed design criteria, while the second frame is identical to the first except for its non-compliant span-to-depth ratio of 4. This ratio was selected because it represents typical tubular frame systems [3]. The third frame implements the proposed NPBS concept to enable a direct comparison with conventional systems. Note that all three frames share identical geometric and material properties, differing only in beam section detailing (RBS vs. NPBS) and span-to-depth ratio to ensure a fair performance comparison. The proposed system was designed based on AISC 341 and AISC 358, and the main seismic detailing requirements were considered, including strong column–weak beam, controlled yielding in the beam region, satisfaction of slenderness limits, beam shear strength checks, and code-consistent design of the beam-to-column connection and panel zone. It is noted that the conventional span-to-depth ratio limitation is not strictly satisfied; this point is discussed as a practical limitation and indicates the need for further validation before wider code implementation.

2-1- Numerical Studies

For the numerical studies in this research, the nonlinear finite element analysis software ABAQUS was utilized [21]. Additionally, the validation of the analytical method was performed based on a specimen experimentally tested by the authors [16]. In this experiment, a conventional moment-resisting frame with reduced beam sections and a clear span-to-depth ratio of 4 was subjected to static loading. These specimens were designed according to code requirements at half-scale for a main frame with 2.8-meter height and 3-meter span, and were modeled in ABAQUS software.

The steel grade ST37 with yield stress of 300 MPa was used for beams, columns, continuity plates, and end plates. To reduce analysis time, the models were simulated using S4R isoparametric shell elements with four nodes. The shell elements are capable of considering local buckling effects. Details of end plates and continuity plates were not modeled, and bolts and welds were not simulated in detail. To improve results and enhance accuracy, especially at connection locations, sensitivity analysis was performed.

The von Mises failure criterion and its rules were used to model plasticity, and a combination of kinematic and isotropic strain hardening was employed to model hardening behavior. The stress-strain curves of members were predicted based on coupon test results and the study by Kaufman et al. In this paper, the researchers proposed a formula for stress-strain curves of steels with specified yield stress. Therefore, materials with properties similar to those mentioned in the study were used to predict the plastic behavior of structural members in this experiment. Steel material properties are obtained through coupon testing according to ASTM E8/EM-16A. Test specimens are tested at a displacement rate of 10 mm/min. Based on the tests, the resultant yield strength of steel is found to be 300 MPa, and the ultimate strength is 370 MPa. The average elastic modulus is 200,000, MPa and the elongation at break is 34%. Moreover, the cyclic material properties are calibrated using the data from Kaufmann et al.'s cyclic coupon tests on Steel C (A572 grade 50 steel) [22].

To simplify the numerical analysis, boundary conditions and loading were considered with minor modifications compared to the experimental specimen. Lateral restraints, which had negligible effect on frame behavior, were not modeled. To account for axial forces in beams, the load application point was alternated in each loading cycle. Specifically, the load was applied alternately to the left and right sides of column tops at beam-column connection height. Additionally, geometric nonlinearity was activated in ABAQUS to consider large displacement effects, enabling simulation of local yielding and post-buckling behavior of members. According to experimental loading conditions, the loading protocol for beam-to-column connections in moment-resisting frames from ANSI/AISC 341-10 [23] was used for analyses.

The finite element models of the moment-resisting frame and shear link frame were rigorously validated against the experimental results. This validation encompasses both global force-displacement response and local failure mechanisms, ensuring a comprehensive assessment of the model's predictive accuracy.

Global Response Comparison: Figure 4 presents a direct comparison between the experimental and numerical hysteretic force-displacement curves for both frame types. The FE models successfully capture all critical behavioral characteristics observed in the tests, including the initial elastic stiffness, yield point, hardening phase, strength degradation, and pinching behavior. Quantitatively, the model demonstrates excellent agreement with the experimental data. The predicted maximum strength shows a negligible error of only 1%, while the deviation in initial stiffness is approximately 6%. These minimal discrepancies confirm the high fidelity of the numerical models in simulating the global structural performance.

Local Failure Mode and Damage Verification: Beyond global response, the accuracy of the model in predicting localized damage is crucial. Figure 5 provides a comparative visual analysis of the final damage state. Figure 5(a) depicts the physical condition of the MRF specimen at the conclusion of the laboratory test, where pronounced plastic hinges have formed at the beam-column connections. Figure

5(b) illustrates the corresponding result from the ABAQUS finite element analysis, visualized through the contour plot of the equivalent plastic strain. The concentration of high PEEQ values in the FE model (shown in red) aligns precisely with the locations of the physical plastic hinges observed in the experiment. This correlation confirms that the numerical model not only replicates the global force capacity but also accurately predicts the correct failure mechanism and the spatial distribution of inelastic deformation.

The synthesis of quantitative metrics (low error in strength and stiffness) and qualitative/visual evidence (matching damage patterns) provides robust verification of the developed FE models. This validated modeling approach establishes a reliable numerical tool for the subsequent parametric studies presented in the following sections.

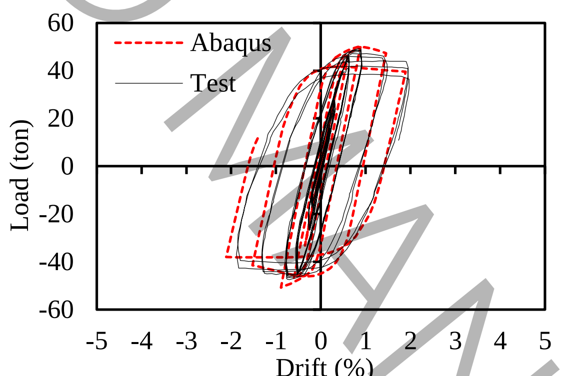

Fig 4: Validation of moment-resisting frame modeling

(a) Laboratory images

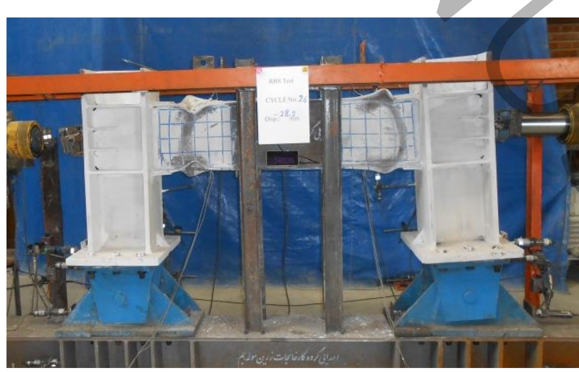

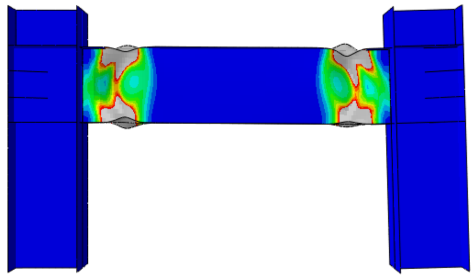

(b) Finite element results

Fig 5: Deformed frame and its yield pattern

Following the validation at this stage, three frames with the aforementioned specifications were designed. The specifications of these three frames, which were designed and modeled based on the validated main frame, are presented in Table 1. As mentioned, these three frames have identical cross-sectional properties and differ only in beam depth and type of section reduction. Considering the beam length of 1200 mm, the beam depth is 170 mm for the frame with span-to-depth ratio of 7 and 300 mm for the ratio of 4. For section reduction in the first two frames, the conventional method was used, while for the third frame, Equation (1) was employed. These three frames were subjected to cyclic static loading, and their seismic characteristics including stiffness, strength, energy absorption, and accumulated plastic strain (PEEQ) were compared.

Table 1: Section Properties of Specimens (Dimensions in mm)

	d	b_f	t_w	t_f
First Beam	170	150	6	8
Second Beam	300	150	6	8
Coulmn	280	280	12	20

3- Results and Discussion

According to the presented content, the three discussed frames were designed and modeled in ABAQUS software. Fig 6, from right to left respectively shows the load-drift ratio diagrams of: a conventional moment-resisting frame with reduced sections at both beam ends and span-to-depth ratio of 7; a conventional moment-resisting frame with reduced sections at both beam ends and span-to-depth ratio of 4; and a moment-resisting frame with non-prismatic reduced sections along the beam length and span-to-depth ratio of 4. As seen in this figure, none of the three frames show stiffness degradation. Furthermore, the moment-resisting frame with non-prismatic reduced sections along the beam length exhibits stable hysteretic behavior until strength degradation occurs. However, strength degradation in the conventional moment-resisting frame with span-to-depth ratio of 4 happens much earlier than in the other frames, indicating the weakness of this frame which was not constructed according to code limitations.

The stiffness values, maximum strength, Equivalent Plastic Strain (PEEQ), and energy absorption of these three frames are presented in Table 2. As can be seen from this table, the maximum strength and stiffness of the two frames with clear span-to-depth ratio of 4 are approximately equal, and the stiffness of the moment-resisting frame with non-prismatic sections has decreased by only 8% compared to the conventional moment-resisting frame with the same depth. Meanwhile, the initial strength and stiffness of the moment-resisting frame with span-to-depth ratio of 7 are more than two times lower than its counterpart with ratio of 4, indicating the weakness of this frame. It should be noted that span-to-depth ratio of 4 is not permitted for conventional moment-resisting frames according to codes.

PEEQ is a scalar variable commonly reported in nonlinear finite element analyses to quantify the accumulated plastic deformation in a material point. It represents the history-dependent measure of plastic straining and is widely used as an indicator of plastic demand and damage concentration in steel components. In this study, PEEQ distributions and peak values are used to compare the extent and localization of inelastic deformation between the reference and the proposed systems.

For better comparison of these three frames, step-by-step and cumulative comparisons of energy absorption and PEEQ were performed. Figures 7 and 8 show the PEEQ status of these three frames. As evident from these figures, the PEEQ of the frame with span-to-depth ratio of 7 and the frame with non-prismatic reduced sections are approximately equal, while the conventional moment-resisting frame with span-to-depth ratio of 4 has about 2.6 times higher PEEQ than these two frames. It should be mentioned that PEEQ is an appropriate criterion for showing increased probability of frame fracture. Moreover, as seen in Fig 7, in conventional systems, yielding occurs only at both ends of the beam, while in the innovative frame of this research, yielding has occurred along a larger portion of the beam length.

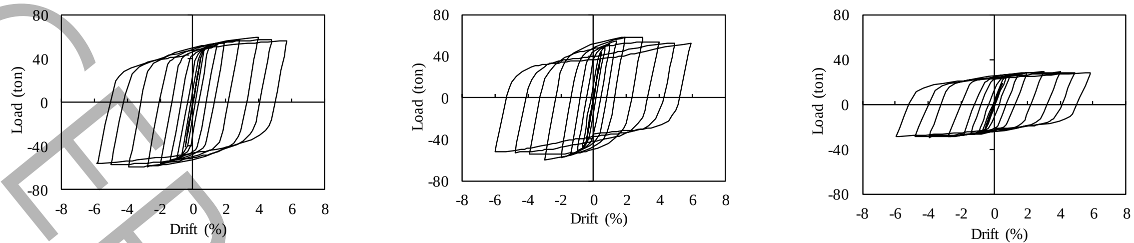

With reduced sections along entire beam length and L/D=4 | With reduced sections at both beam ends and L/D=4 | With reduced sections at both beam ends and L/D=7

Fig 6: Load-drift ratio diagrams of moment-resisting frames

Table 2: Comparison of seismic characteristics of the frames.

	Stiffness (Kn/m)	Peak Strength (Kn)	PEEQ	Dissipated energy (MJ)
First System	393	291	0.568	15.7
Second System	920	584	1.469	30.2
Third System	848	596	0.558	32.1

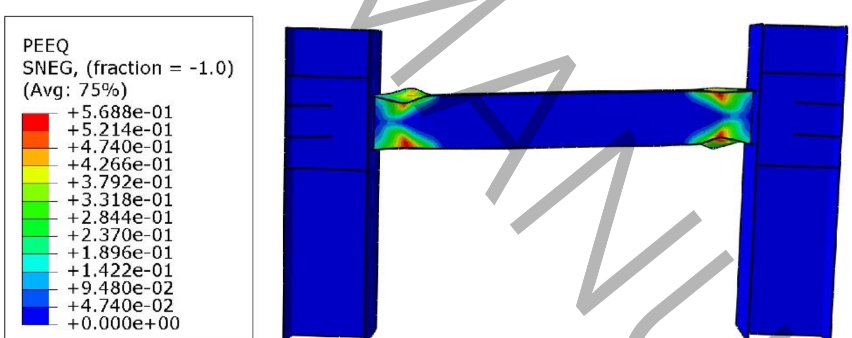

(a) With reduced sections at beam ends and L/D=7

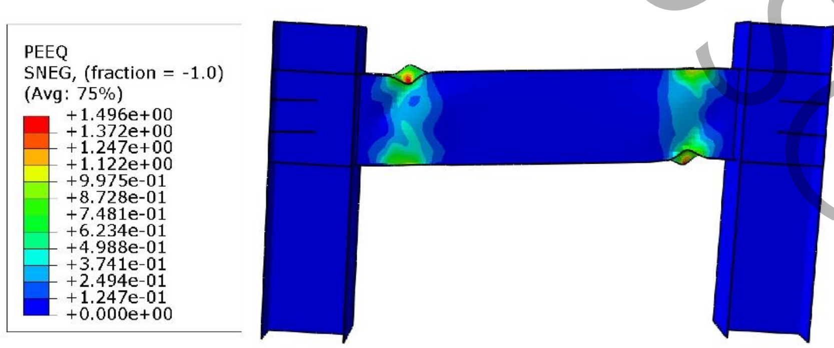

(b) With reduced sections at beam ends and L/D=4

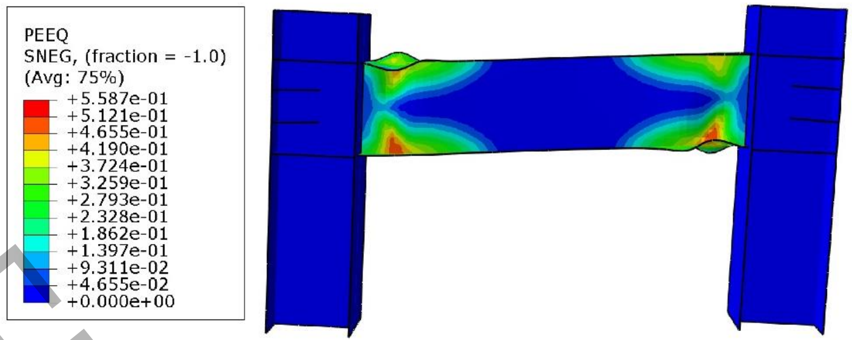

(c) With non-prismatic reduced sections along beam length and L/D=4

Fig 7: Frame deformation at 6% drift:

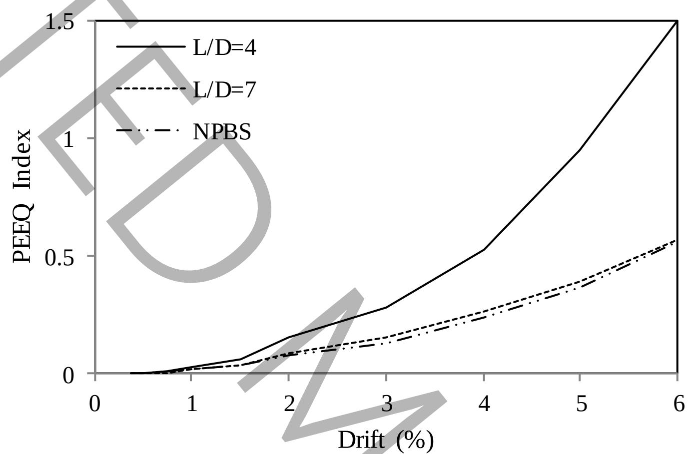

Fig 8: Maximum Equivalent Plastic Strain (PEEQ) at different drift levels

In addition to the previously mentioned characteristics, energy absorption is another feature examined in this study. Besides Table 2 which shows the cumulative energy absorption of these three frames, Fig 9 records the energy absorbed by these three frames at different drift percentages. According to the results, the frame with non-prismatic reduced sections along the beam length absorbs the most energy among these three frames. The conventional frame with span-to-depth ratio of 4 absorbs less energy than this frame, while the frame with ratio of 7 absorbs less than half of these two frames, indicating its weakness compared to the other two frames. Thus, it can be concluded that the frame with non-prismatic reduced sections along the beam length performs better than conventional frames. Besides the superiority of the frame with the proposed idea in this paper over conventional frames, it should be noted that this idea can also be used for retrofitting existing frames where the code-specified span-to-depth ratio limit has not been observed.

As evident from the aforementioned tables and figures, the frame with non-prismatic reduced sections has nearly identical energy absorption, strength and stiffness compared to the conventional frame with reduced sections, but the conventional frame shows about three times higher plastic strain PEEQ, indicating increased fracture risk. The proposed system exhibits a lower equivalent plastic strain (PEEQ) compared to the reference configuration, which can be explained by changes in the plastic deformation pattern and internal force distribution. First, the proposed approach promotes distributed yielding, whereby plastic deformation is spread over an extended region rather than being concentrated within a short segment. This redistribution prevents plastic strain accumulation at a single critical location and reduces peak PEEQ values. Second, the modified geometry and stiffness distribution in the proposed configuration reduces stress concentration effects at critical beam regions. By avoiding abrupt stiffness discontinuities, the system mitigates localized strain intensification, resulting in a smoother stress/strain field and lower PEEQ accumulation. Third, yielding in the proposed system occurs through a progressive yielding mechanism, where yielding initiates locally and then gradually develops across the designed region as the loading increases. This gradual activation leads to a more stable inelastic response and prevents sudden formation of a highly localized plastic hinge, thereby reducing concentrated plastic strain demand. Finally, due to the altered distribution of stiffness and strength, the proposed configuration reduces the flexural demand at beam ends and delays severe end plastic hinge development. Since beam-end plastic hinges are typically associated with high curvature and large plastic strain accumulation, limiting their severity directly contributes to the observed reduction in PEEQ and overall plastic damage concentration. Therefore, converting conventional reduced sections to non-prismatic reduced sections appears to be an appropriate method for performance improvement and retrofitting.

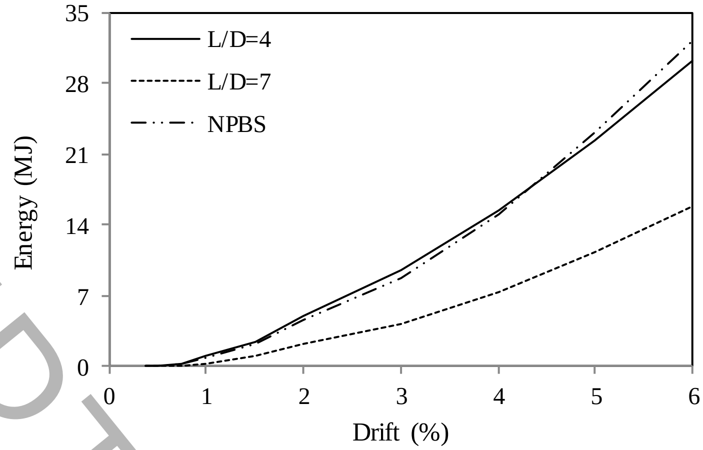

Fig 9: Energy absorbed at different drift levels.

While the present study focuses on evaluating the proposed concept at the beam/frame level to clarify the underlying inelastic mechanism and performance improvement, extending the investigation to multi-story moment-resisting frames (low-, mid-, and high-rise) is an important next step. Such studies are expected to provide further insight into system scalability, inter-story drift distribution, global stability, and the interaction between story-wise demand and the distributed yielding mechanism. This extension is currently being pursued by the authors and will be reported in future work

4- Conclusions

This paper presents an innovative approach of reducing beam sections along the entire length of moment-resisting frames. The proposed method not only maintains system stiffness but also satisfies code requirements regarding minimum clear span-to-depth ratios for beams. According to seismic codes, intermediate and special moment frames must maintain span-to-depth ratios of 5 and 7, respectively.

To evaluate the system's performance, three frame types were analytically investigated: (1) a moment frame with span-to-depth ratio of 7 and reduced beam sections at both ends, (2) a moment frame with span-to-depth ratio of 4 and reduced beam sections at both ends, and (3) a moment frame with span-to-depth ratio of 4 and non-prismatic reduced sections along the beam length. The systems were designed according to code provisions at half-scale, representing a prototype frame with 2.8 m height and 3 m span, and modeled in ABAQUS. These models underwent static cyclic loading to assess their strength, stiffness, plastic strain, and energy absorption capacities.

Results indicate that, as expected, the frame with span-to-depth ratio of 7 showed minimum stiffness among the systems, while the frame with span-to-depth ratio of 4 and end reduced sections exhibited maximum stiffness. However, the critical finding is that the frame with span-to-depth ratio of 4 and end reduced sections developed approximately 2.5 times greater plastic strain than the other systems. The proposed system with non-prismatic reduced sections along the beam length not only resolves stiffness issues but also demonstrates significantly lower plastic strain compared to conventional systems, while eliminating the need to comply with code-mandated minimum span-to-depth ratios.

In summary, compared to conventional frames with span-to-depth ratio of 7, the proposed frame shows approximately 2.15 times greater stiffness, twice the strength, double the energy absorption, and equivalent plastic strain. When compared to conventional frames with span-to-depth ratio of 4 (which violates code requirements), the proposed system maintains similar stiffness, strength and energy absorption, but with only 37% of the cumulative plastic strain, demonstrating the superiority of the proposed concept. This innovative approach proves particularly applicable to tubular systems where perimeter frames are designed to resist lateral loads. The system maintains code-compliant performance while overcoming span-to-depth ratio limitations common in such structural configurations.

References

[1] M. Bruneau, C. M. Uang, and R. Sabelli, Ductile design of steel structures. Boston: McGraw-Hill, 2011.

[2] AISC (American Institute of Steel Construction), "'Prequalified connections for special and intermediate steel moment frames for seismic applications.' ANSI/AISC 358-16," Chicago, 2016.

[3] B. S. Taranath, Structural analysis and design of tall buildings: Steel and composite construction. Boca Raton: CRC Press, 2011.

[4] J. Shen, T. Kitjasateanphun, and W. Srivanich, "Seismic performance of steel moment frames with reduced beam sections," Eng. Struct., vol. 22, no. 8, pp. 968–983, Jun. 2000, doi: 10.1016/S0141-0296(99)00048-6.

[5] H. Nazaralizadeh, H. Ronagh, P. Memarzadeh, and F. Behnamfar, "A practical design approach to bolted end-plate vertical-slits RWS connection," Bull. Earthq. Eng., vol. 20, no. 1, pp. 547–586, Jan. 2022, doi: 10.1007/s10518-021-01238-2.

[6] R. Ahmady Jazany, “Improved design of drilled flange (DF) moment resisting connection for seismic regions,” Bull. Earthq. Eng., vol. 16, no. 5, pp. 1987–2020, May 2018, doi: 10.1007/s10518-017-0265-9.
[7] M. A. Morshedi, K. M. Dolatshahi, and S. Maleki, “Double reduced beam section connection,” J. Constr. Steel Res., vol. 138, pp. 283–297, Nov. 2017, doi: 10.1016/j.jcsr.2017.07.013.
[8] A. Saleh, S. R. Mirghaderi, and S. M. Zahrai, “Cyclic testing of tubular web RBS connections in deep beams,” J. Constr. Steel Res., vol. 117, pp. 214–226, Feb. 2016, doi: 10.1016/j.jcsr.2015.10.020.
[9] M. Gerami, H. Saberi, V. Saberi, and A. Saedi Daryan, “Cyclic behavior of bolted connections with different arrangement of bolts,” J. Constr. Steel Res., vol. 67, no. 4, pp. 690–705, Apr. 2011, doi: 10.1016/j.jcsr.2010.11.011.
[10] K. M. McMullin and A. Astaneh-Asl, “Steel Semirigid Column–Tree Moment Resisting Frame Seismic Behavior,” J. Struct. Eng., vol. 129, no. 9, pp. 1243–1249, Sep. 2003, doi: 10.1061/(ASCE)0733-9445(2003)129:9(1243).
[11] P. Sultana and M. A. Youssef, “Seismic performance of modular steel frames equipped with shape memory alloy braces,” Bull. Earthq. Eng., vol. 16, no. 11, pp. 5503–5527, Nov. 2018, doi: 10.1007/s10518-018-0394-9.
[12] H. Peng, J. Ou, A. Schellenberg, F. Mckenna, and S. Mahin, “Seismic Behavior of Steel Moment Frames with Mechanical Hinge Beam-to-Column Connections,” Int. J. Struct. Stab. Dyn., vol. 20, no. 06, p. 2040005, Jun. 2020, doi: 10.1142/S0219455420400052.
[13] M. T. Nikoukalam and K. M. Dolatshahi, “Finite element investigation of moment resisting frames with a new shear structural fuse,” in Second European Conference on Earthquake Engineering and Seismology, 2014.
[14] S. R. Mirghaderi, B. Mahmoudi, A. Gharavi, K. M. Dolatshahi, and S. Epackachi, “Experimental investigation of moment resisting frames with perforated shear link,” Structures, vol. 32, pp. 516–531, Aug. 2021, doi: 10.1016/j.istruc.2021.03.060.
[15] K. M. Dolatshahi, A. Gharavi, and S. R. Mirghaderi, “Experimental investigation of slitted web steel moment resisting frame,” J. Constr. Steel Res., vol. 145, pp. 438–448, 2018.
[16] F. Mahmoudi, K. M. Dolatshahi, M. Mahsuli, M. T. Nikoukalam, and A. Shahmohammadi, “Experimental study of steel moment resisting frames with shear link,” J. Constr. Steel Res., vol. 154, pp. 197–208, Mar. 2019, doi: 10.1016/j.jcsr.2018.11.027.
[17] F. Mahmoudi and P. Tehrani, “A Technique for Seismic Rehabilitation of Damaged Steel Moment Resisting Frames,” J. Rehabil. Civ. Eng., vol. 8, no. 4, pp. 106–117, 2020.
[18] F. Mahmoudi, K. M. Dolatshahi, M. Mahsuli, A. Shahmohammadi, and M. T. Nikoukalam, “Experimental Evaluation of Steel Moment Resisting Frames with a Nonlinear Shear Fuse,” in Geotechnical and Structural Engineering Congress 2016, 2016, pp. 624–634, doi: 10.1061/9780784479742.052.
[19] M. Lian, B. Guan, Q. Cheng, H. Zhang, and M. Su, “Experimental and numerical study of seismic performance of high-strength steel fabricated framed-tube structures with replaceable shear links,” Structures, vol. 28, pp. 2714–2732, Dec. 2020, doi: 10.1016/j.istruc.2020.10.081.
[20] B. Guan, M. Su, and M. Lian, “Seismic behaviour of combined steel framed-tube substructure with replaceable shear links,” J. Constr. Steel Res., vol. 167, p. 105968, Apr. 2020, doi: 10.1016/j.jcsr.2020.105968.
[21] SIMULIA, “Abaqus analysis user’s manual,” The Dassault Systèmes, Realistic Simulation. USA, 2014.
[22] E. Kaufmann, B. Metrovich, and A. Pense, “Characterization of cyclic inelastic strain behavior on properties of A572 Gr. 50 and A913 Gr. 50 rolled sections,” 2001.
[23] AISC (American Institute of Steel Construction), “‘Seismic provisions for structural steel buildings.’ AISC/ANSI 341-16,” Chicago, 2016.